ACS chemical biology

Articles

pubs.acs.org/acschemicalbiology

Insights into the Glycosaminoglycan-Mediated Cytotoxic Mechanism of Eosinophil Cationic Protein Revealed by NMR

M. Flor García-Mayoral,[†] Ángeles Canales,[‡] Dolores Díaz,[§] Javier López-Prados,[∥] Mohammed Moussaoui,[⊥] José L. de Paz,[∥] Jesús Angulo,[∥] Pedro M. Nieto,[∥] Jesús Jiménez-Barbero,[§] Ester Boix,[⊥] and Marta Bruix*[,†]

[†]Departamento de Química Física Biológica, Instituto de Química Física Rocasolano, CSIC, Madrid, Spain

[‡]Departamento de Química Orgánica I, Facultad de Ciencias Químicas, Universidad Complutense, Madrid, Spain

[§]Departamento de Biología Físico Química, Centro de Investigaciones Biológicas, CSIC, Madrid, Spain

[∥]Departamento de Química Orgánica y Biológica, Instituto de Investigaciones Químicas, CSIC-Universidad de Sevilla, Sevilla, Spain

[⊥]Departamento de Bioquímica y Biología Molecular, Facultad de Biociencias, Universidad Autónoma de Barcelona, Barcelona, Spain

Supporting Information

ABSTRACT: Protein-glycosaminoglycan interactions are essential in many biological processes and human diseases, yet how their recognition occurs is poorly understood. Eosinophil cationic protein (ECP) is a cytotoxic ribonuclease that interacts with glycosaminoglycans at the cell surface; this promotes the destabilization of the cellular membrane and triggers ECP's toxic activity. To understand this membrane destabilization event and the differences in the toxicity of ECP and its homologues, the high resolution solution structure of the complex between full length folded ECP and a heparin-derived trisaccharide (*O*-iPr-α-D-GlcNS6S-α(1−4)-L-IdoA2S-α(1−4)-D-GlcNS6S) has been solved by NMR methods and molecular dynamics simulations. The bound protein retains the tertiary structure of the free protein. The $^{2}S_{0}$ conformation of the IdoA ring is preferably recognized by the protein. We have identified the precise location of the heparin binding site, dissected the specific interactions responsible for molecular recognition, and defined the structural requirements for this interaction. The structure reveals the contribution of Arg7, Gln14, and His15 in helix α1, Gln40 in strand β1, His64 in loop 4, and His128 in strand β6 in the recognition event and corroborates the previously reported participation of residues Arg34−Asn39. The participation of the catalytic triad (His15, Lys38, His128) in recognizing the heparin mimetic reveals, at atomic resolution, the mechanism of heparin's inhibition of ECP's ribonucleolytic activity. We have integrated all the available data to propose a molecular model for the membrane interaction process. The solved NMR complex provides the structural model necessary to design inhibitors to block ECP's toxicity implicated in eosinophil pathologies.

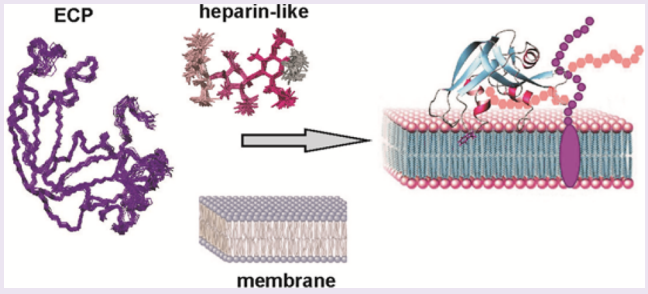

Cytotoxicity is one of the most interesting and least understood properties of several members of the RNase A superfamily. Onconase, a cytotoxic RNase from frogs, became the first member of this superfamily to be assayed for clinical efficacy for anticancer therapy and has reached phase III trial in malignant mesothelioma, as well as phase I/II trial in non-small cell lung cancer.[1] Human eosinophil cationic protein (ECP)/RNase 3, another member of this protein superfamily, shares the same topology and fold of RNase A and conserves the same catalytic triad and disulfide bonds. Despite these similarities, their biological functions greatly differ: ECP is an intrinsically poor RNase for common RNA substrates compared to RNase A yet is highly toxic, a property that RNase A lacks.[2−4]

ECP is found in the specific secondary granules of eosinophils. The protein is secreted by activated eosinophil granulocytes during infection, acting as a mediator in the human immune host defense response.[4,5] ECP's toxicity has been reported against a wide spectrum of pathogens, ranging from viruses and bacteria to helminth and protozoa parasites.[6,7] Unfortunately, ECP secretion is also linked to pathogenesis.[8] For example, ECP's toxicity would contribute to cerebral malaria and liver fibrosis, a major cause of schistosomiasis morbidity.[4] The protein's toxicity was analyzed on brain cell cultures and related to apoptosis.[9] Except for the antiviral action[10] and neurotoxicity, the cytotoxic effect of ECP seems to be independent of the RNase activity.[11] ECP is cytotoxic to host epithelial tissues such as the tracheal and bronchial epithelium,[12,13] and growth inhibition effects have been described for different mammalian cell lines.[14−16]

ECP's cytotoxicity is the subject of intense research due to the tissue damage associated to eosinophil degranulation at the inflammation site.[6,17] Novel eosinophil targeting therapies are

Received: July 25, 2012
Accepted: October 1, 2012
Published: October 1, 2012

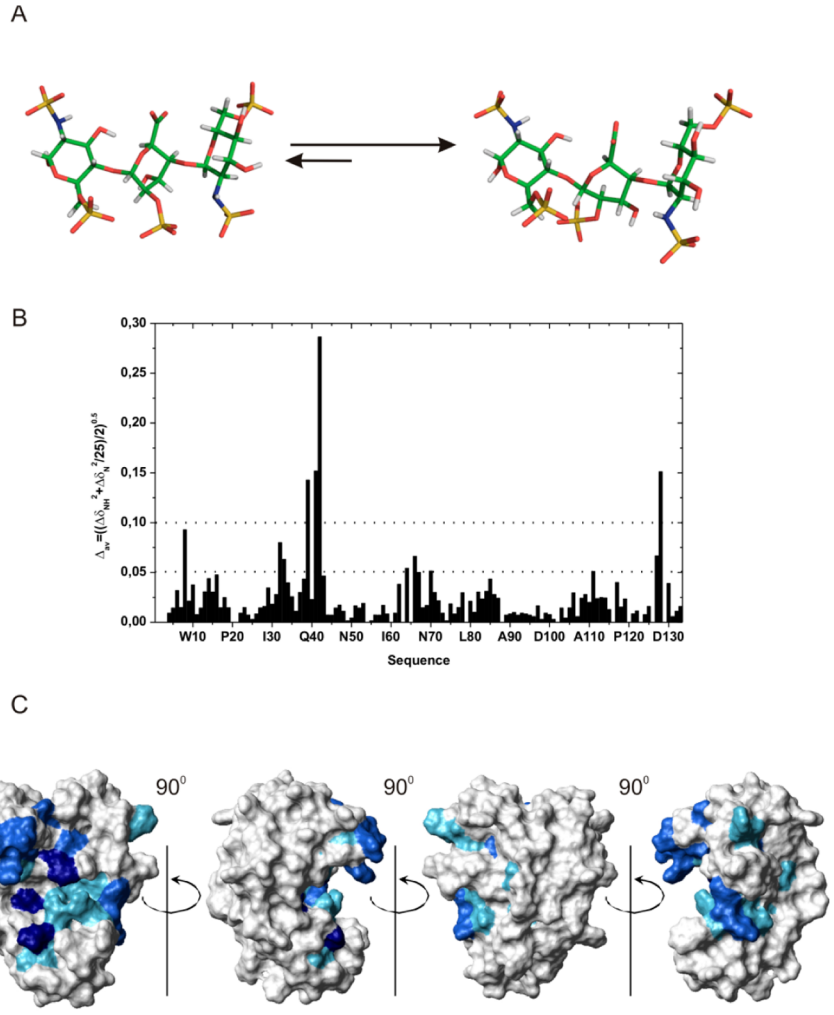

Figure 1. (A) A view of the trisaccharide [*O*-iPr-α-D-GlcNS6S-α(1−4)-L-IdoA2S-α(1−4)-D-GlcNS6S] used in this study, showing the chair ($^1C_4$)−skew-boat ($^2S_0$) equilibrium of the IdoA ring. (B) Plot of the weighted average of amide ^{15}N and ^1H chemical shift variations of ECP upon binding to the trisaccharide. (C) Mapped surface of the ECP interaction with the trisaccharide heparin mimetic based on the averaged chemical shift perturbations. The color code refers to the magnitude of the chemical shift perturbation values: navy blue for residues with values >0.1 ppm, royal blue for residues with values 0.05 < x <0.1 ppm, and sky blue for residues with values 0.03 < x <0.05 ppm.

under development,[18] and the anti-inflammatory properties of heparin derivatives are a promising research field.[19] The protein's toxicity on host tissues is attributed to its ability to bind to the cell surface and to promote the destabilization of the cytoplasmic membrane. High affinity binding for glycosaminoglycans (GAGs) at the cell surface is critical for triggering the initial step of this process.[14,20,21] Also a protein surface rich in positive charge is essential for this activity.[22]

The structure of ECP has been solved by NMR[23] and X-ray methods, in the absence[24,25] and the presence of sulfate anions,[26] as well as its complex with 2′,5′-ADP.[27] Here we combine the NMR spectroscopy with docking and MD simulations to obtain the high resolution solution structure of the complex between enzymatically active ECP and a heparin-derived trisaccharide, and we dissect the specific interactions responsible for the molecular recognition. A few GAG binding proteins, most cocrystallized with heparin oligosaccharides, have been deposited in the PDB. Only the complex structure of human FGF-1 with a hexasaccharide heparin analogue has been solved in solution by NMR spectroscopy.[28] To the best of our knowledge this is the first reported structure of an RNase A protein family member with a GAG. The solved NMR complex provides the structural basis to assist the design of inhibitors of the protein's toxicity to host tissues associated to eosinophilia pathologies and inflammation processes. In a wider context, binding to heparan sulfate proteoglycans (HSPGs) plays a key role in cell recognition pathways and is a priority focus of the pharmaceutical industry to intracellular targeting.[29,30]

RESULTS AND DISCUSSION

Heparin-derived oligosaccharides are good models for the study of protein−membrane interactions, since they mimic the sulfated domains of heparan sulfate (HS). Diverse biochemical, biophysical, and mutational studies have focused on the identification of the regions of ECP important for the high affinity binding to heparin oligosaccharides, highlighting the importance of the Trp residues[14] and loop 3 residues Arg34−Asn39.[31,32] However, the atomic description of the binding site and the specific intermolecular interactions established were not known in detail as no high resolution structures of folded ECP with heparin mimetics have been solved to date.

Bound Structure of ECP. We proved the interaction of ECP and the synthetic chemically well-defined trisaccharide heparin mimetic (Figure 1A) by NMR (Supporting Figure S1)

dx.doi.org/10.1021/cb300386v | *ACS Chem. Biol.* 2013, 8, 144−151

and found that residues most affected by the complex formation (Figure 1B,C) are concentrated into nonsequential but localized regions.

For comparison, Figure 2 shows the superposition of the 20 lowest-energy structures of the calculated family of ECP in the

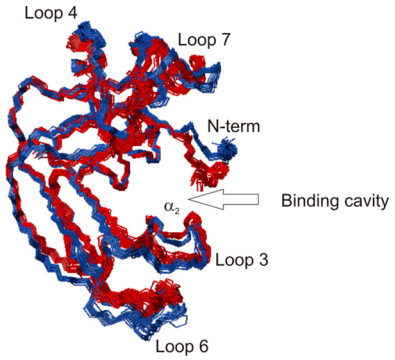

Figure 2. Superposition of the lowest-energy families of 20 conformers of the free (red) (PDB: 2KB5) and bound conformations of ECP (blue) (determined in this study). The elements of structure that experience the major structural differences are labeled.

complex with those of the free protein (PDB: 2KB5). The structure retains the same fold and the similar structural features of the previously described free protein[23] (Supporting Table S1) as in many other complexes. This contrasts with the interaction of antithrombin III with heparin[33] where a significant conformational change leads to the exposure of the reactive site loop for factor Xa recognition and promotion of inhibition. In ECP, subtle changes are localized on the side of the molecule bearing the carbohydrate binding groove. Variations are located in loops 3, 4, 6, and 7, the N-terminus, and helix α2. The movement of the N-terminus away from loop 3 produces a widening of the entrance to the binding cavity and facilitates the accommodation of the carbohydrate. Since residues at the N-terminus and loop 6 were found to be selectively affected by ECP binding to DPC micelles,[32] changes induced by the trisaccharide in the conformation of these regions might be important to promote the interaction with the membrane.

Model Structure of the Trisaccharide Heparin Mimetic. The synthetic trisaccharide used in this work adequately reproduces the conformational equilibrium between the $^2S_0$ and $^1C_4$ conformers of the central IdoA ring (Figure 1A), as well as the 3D flat helix structure of heparin.[34,35] In addition, the sulfate groups point to opposite sides of the central saccharide core as they do in the 3D structure of heparin.[36] We added an isopropyl group to fully populate the α-anomer, which is present in natural heparin.[37] Two structures were calculated for the two most representative conformations of the IdoA2S ring, the $^2S_0$ and the $^1C_4$. The structure of the trisaccharide generated with the $^2S_0$ IdoA pyranose ring conformation was chosen as the most representative to model the complex, since the intense $^2S_0$-exclusive NOE between the H2 and H5 protons in the ECP-bound trisaccharide was observed (data not shown).

ECP-Trisaccharide Heparin Mimetic Complex Binding Affinity. We have estimated the dissociation constant of the ECP-trisaccharide heparin mimetic complex from the titration curve plots of a set of well-dispersed NMR signals perturbed by the interaction (Figure 3). The values obtained are in the low micromolar range (15−30 μM), and the interaction occurs on the fast (sub millisecond) exchange regime. Dissociation constants in this range have been reported for other heparin oligosaccharide complexes.[38,39] The values here determined are larger than that reported for ECP bound to low molecular weight heparin (<150 nM),[40] providing evidence that an increase of the oligosaccharide length strengthens the interactions.

Structure of the ECP-Trisaccharide Heparin Complex. Few intermolecular NOEs could be detected as is usually the case with protein-oligosaccharide complexes.[41] Nevertheless, unambiguous NOEs could be assigned among the Gln40 side chain Hβ, Hγ, and Hε protons and the H2 and H4 protons of the GlcNS (**C**) ring. These cross peaks allowed us to definitively orient the non-reducing end of the trisaccharide toward the interior of the ECP's carbohydrate binding site. Also, an assigned intermolecular NOE between the isopropyl group attached to the reducing end GlcNS (**A**) ring and the Qδ protons of Arg7 is consistent with this orientation. Intermolecular NOEs involving the charged end of the long side chains of Arg and Lys residues are commonly observed in this type of complexes.[28,42]

Figure 4A shows the superposition of the 20 conformer family obtained after 75 ps of MD simulation. Figure 4B gathers 20 conformers selected as a representative family following 3 ns of simulation. It is clearly observable that the carbohydrate orientation within the binding channel, as well as the position of the sulfate and carboxylate groups, is considerably better defined in the 3 ns simulation relative to the 75 ps calculation. In the ensemble from the 75 ps simulation runs, the variability of these groups is larger, but importantly, they still cluster with similar average orientations. The *N*-sulfate of GlcNS (**A**), the carboxylate in position 6 of IdoA (**B**), and the 6-*O*-sulfate of GlcNS (**C**) point toward the helix α1, while the 6-*O*-sulfate of GlcNS (**A**), the 2-*O*-sulfate of IdoA (**B**), and the *N*-sulfate of GlcNS (**C**) point toward loop 3. Since the analysis of the representative family from the 3 ns dynamics gave a larger number of structures with the atoms of GlcNS (**C**) closer to Gln40, we selected one conformer from this family to further detail the molecular interactions that are important for the recognition and for the stability of the complex. The analysis of the fluctuations of selected intermolecular distances along the 3 ns trajectory is represented in Supporting Figures S2−S3.

Heparin binding sites have been found to be diverse and not restricted to specific secondary structure elements. For instance, compared to the complex structures of FGF-1[28] and the C-type lectin eosinophil protein EMBP[43] bound to heparin saccharides, where the binding site resides in solvent-exposed loops, ECP's binding site is significantly less accessible, which presumably explains the necessity for the N-terminus displacement at the entry of the binding cavity. Similarly, the E2 domain of APLP1 bound to a heparin tetrasaccharide is snugly bound inside a narrow groove formed in this particular case by the two helical subdomains of one protein protomer.[44] The ECP heparin's binding site consists of a positively charged groove that runs parallel to strand β6, the edges of which are delimitated by helix α1 and loop 3 on each side and strand β1 on top. Similarly to all reported complexes with heparin polysaccharides, most of the contacts established between ECP and the trisaccharide heparin mimetic are electrostatic in nature, revealing that charge complementarity is necessary for binding (Figure 5). The *N*-sulfate of GlcNS (**A**) participates in salt bridge interactions with the guanidinium groups of Arg7

dx.doi.org/10.1021/cb300386v | *ACS Chem. Biol.* 2013, 8, 144−151

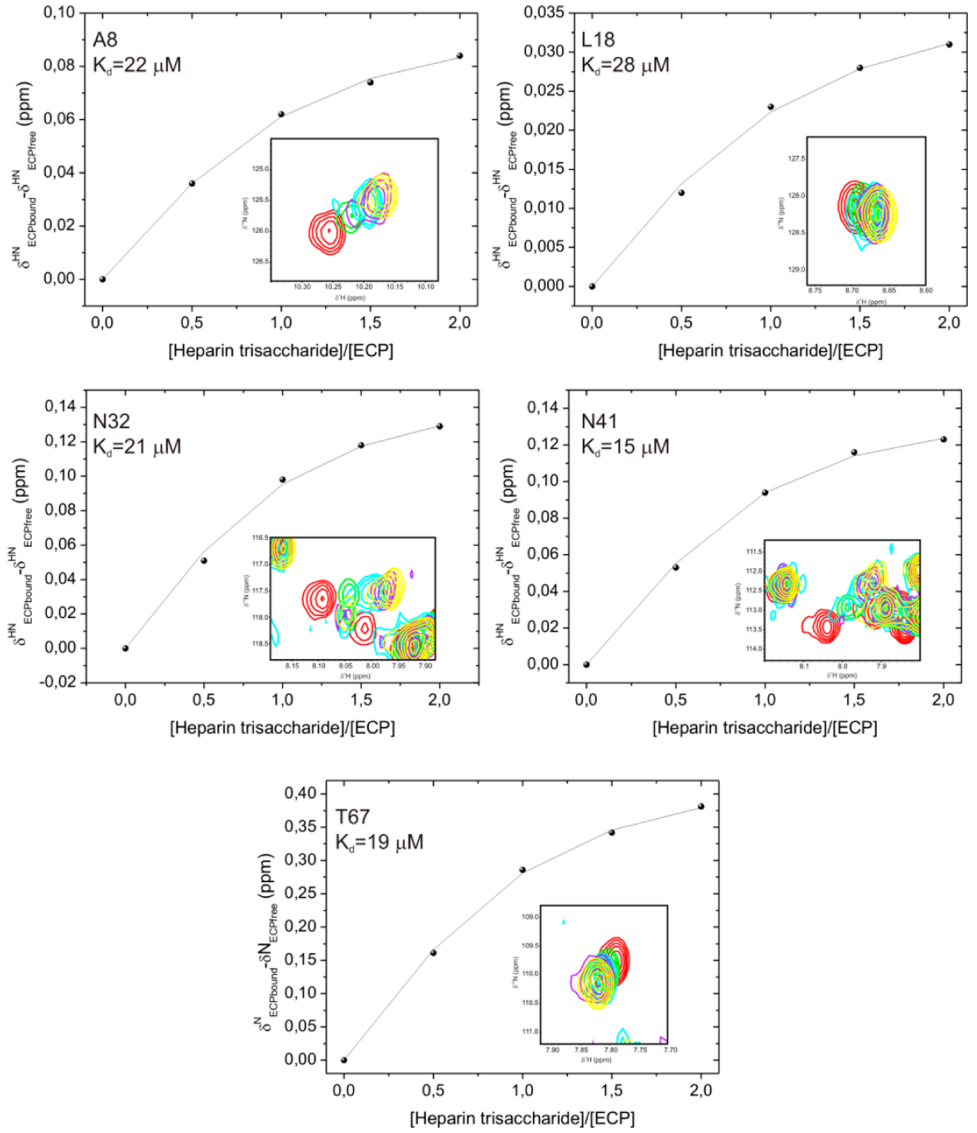

Figure 3. Determination of the dissociation constant of the ECP-heparin trisaccharide complex. Plots of several titration curves from selected perturbed residues and fits to the 1:1 binding model are shown. The insets represent the shifts from selected resonances along the titration at the different ECP-carbohydrate ratios: red, 1:0; green, 1:0.5; cyan, 1:1; purple, 1:1.5; yellow, 1:2.

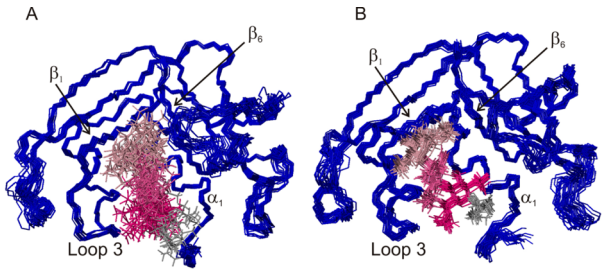

Figure 4. Superposition of the 20 conformers of the ECP-trisaccharide heparin mimetic complex obtained from (A) the 75 ps dynamics and (B) the 3 ns dynamics. The protein backbone is colored in blue, the different saccharide units in different shades of pink, and the isopropyl group in gray.

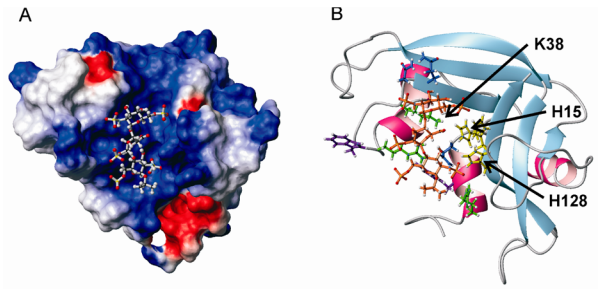

Figure 5. (A) A representative conformer of the ECP-trisaccharide heparin mimetic complex obtained from the 3 ns molecular dynamics. The electrostatic surface is represented for the protein, and the trisaccharide is shown with a ball and stick representation. (B) Details of the intermolecular interactions responsible for ECP recognition of the trisaccharide heparin mimetic. Args and Lyss are colored in green, His in yellow, Trps in purple, Glns and Asns in blue, and the trisaccharide backbone in brown. Catalytic side chains are labeled. ECP is in a ribbon representation.

and Arg34 and electrostatic interactions with the amide side chain group of Gln14, the imidazole rings of His15 (Hε2) and His128 (Hδ1), and the indole ring of Trp10 (Hε1). Some oxygen atoms of the 6-*O*-sulfate are relatively close to the Hε1 of Trp10 and the HN of Trp35, and also short distances exist

dx.doi.org/10.1021/cb300386v | *ACS Chem. Biol.* 2013, 8, 144–151

with the guanidinium of Arg34, in particular to the Hε proton. With respect to the 2-*O*-sulfate of the IdoA (**B**) ring, there are short distances to the Hε1 of Trp35; however, most of the electrostatic contacts involving this pyranose ring are established with the carboxylate in position 6, which interacts with the Hε2 imidazole ring protons of His15 and His128 and forms salt bridges with the amino group of Lys38. Very few contacts are observed with the guanidinium of Arg34. Finally, the *N*-sulfate of GlcNS (**C**) is close to the HN and amide protons of Gln39 and the HN of Asn40. The 6-*O*-sulfate is mainly involved in interactions with the Hδ1 and Hε2 protons of the imidazole ring of His64. Also some hydrogen bonds are formed in most of the structures of the representative family, most of them involving the GlcNS (**A**) ring, such as those between the N-sulfate and the guanidinium of Arg7, the amide side chain of Gln14 and the Hδ1 of His128, and the one between the 6-*O*-sulfate and the Hε of Arg34. The *N*-sulfate of GlcNS (**C**) also establishes a hydrogen bond with the backbone amide of Asn39. No stacking interactions are observed between aromatic rings of Phe or Tyr and the pyranose rings of the carbohydrate, as commonly observed in the recognition of neutral sugars by proteins.[45]

The side chains of Arg7 and Arg34 become much more ordered in the complex, and adopt a unique and defined orientation that facilitates the formation of multiple contacts with the carbohydrate. Similarly to the free protein, the side chain of Trp35 is disordered as corresponds to its high solvent exposure, but its orientation differs greatly. The side chain of His64 is better defined in the complex, and His82 adopts an approximate perpendicular orientation. The side chain of the catalytic His128 differs slightly in the complex. It preserves the overall orientation but shifts to some extent to enable hydrogen bond formation with the ligand. The other catalytic residues, Gln14 and His15, preserve similar orientations of their side chains as in the nonbound ECP, while the side chain of Lys 38 shifts to optimize contacts with the IdoA unit.

It is interesting that His15, Lys38, and His128, in addition to their direct involvement in binding the oligosaccharide, constitute the catalytic triad responsible for ECP's ribonucleolytic activity. Moreover, Arg7, Asn39, Gln40, and His64 are thought to aid catalysis as they were ascribed to putative phosphate secondary binding sites.[24,27] Therefore, this NMR structure explains at atomic resolution why heparin inhibits the RNase catalytic activity.[40]

From the point of view of the trisaccharide we analyzed the glycosidic dihedral angles of the two different GlcNS-IdoA and IdoA-GlcNS linkages (Supporting Figure S4), which have been reported to vary within a narrow range in previously solved complexes.[41] Here, we obtained a well-defined and stable dihedral angle distribution with average values of −50° and −60° for Ψ and Φ, respectively (GlcNS-IdoA), and of 5° and 45° for Ψ and Φ, respectively (IdoA-GlcNS), which are similar to those found in other heparin-protein complexes[41,44] and in the solution conformation of heparin.[46] It is well-known that protein binding may influence the IdoA ring conformational equilibrium selecting one specific conformation upon complex formation. We have studied this equilibrium for the trisaccharide IdoA pyranose ring in the complex during the 3 ns molecular dynamics trajectory by monitoring the distances between the H2 and H5 protons, which are those closer in the $^2S_0$ conformation (Supporting Figure S2A). Interestingly, at the very beginning of the trajectory, up to ∼200 ps, the ring is maintained in the $^2S_0$ form used in the starting model, then jumps to the $^1C_4$ conformation for a large part of the time, and finally at ∼2000 ps returns to the $^2S_0$conformation, which is consistent with the intense experimental H2−H5 NOE observed in the complex. These results corroborate that the $^2S_0$ conformation of the IdoA (**B**) ring is the one preferentially recognized by the protein. The GlcNS rings are less dynamic and remain stable in the preferred $^4C_1$ conformation. We can hypothesize that this geometry may enable specific interactions with the clusters of positive residues on the surface of the protein and contribute to a better fit enhancing the binding affinity.

Recently, a new crystal structure of ECP in the presence of lithium sulfate has been solved and revealed the presence of three main sulfate interacting sites, S1, S2, and S3, at the catalytic groove.[26] The comparison of the position of these sulfates with those in the structure of the ECP-trisaccharide heparin mimetic reveals a general good match, although some minor differences are present as discussed in the Supporting Information.

Molecular Model for the ECP-Membrane Interaction. In order to improve our understanding of the still unclear cytotoxic mechanism of ECP and on the basis of the reported structure, we have examined specific residues and their possible roles, either individually or collectively in the destabilization of lipid membranes. We have integrated all the available results to propose a molecular model for the membrane interaction process (Figure 6).

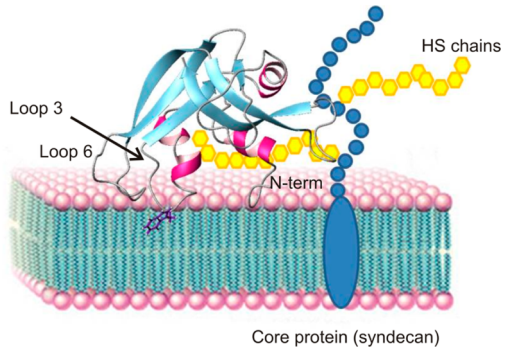

Figure 6. Model of the interaction of ECP with the mammalian cell membrane. The core protein to which the HS is attached is represented in blue, and the different HS chains are colored in yellow. One of these chains is placed in the heparin binding cavity determined for the trisaccharide heparin mimetic. The N-terminal region and loops 3 and 6 that have been shown to participate in the interaction with DPC micelles have been oriented toward the membrane surface, and the solvent-exposed Trp35 residue is shown in purple in an optimal orientation to interact with the phospholipid bilayer.

Following ECP release from the eosinophil granule, the electrostatically driven interactions between the clusters of positively charged residues and the highly sulfated cell surface HSPGs would lead the first step of the mechanism involving "GAG recognition and approach to the membrane". The electrostatic nature of this first stage has been confirmed by its sensitivity to the presence of salt and by the lack of activity on neutral liposomes as membrane models.[47] The ionic interactions are mainly mediated by Arg7, His15, Arg34, Lys38, and His128 and polar contacts with Gln14, Asn39, and Gln40. These interactions would not only promote ECP's approach and binding to the biological membrane but would

dx.doi.org/10.1021/cb300386v | *ACS Chem. Biol.* 2013, 8, 144−151

also facilitate an increase in the local concentration of ECP on the surface.

Once the initial contacts are formed, they can be strengthened by means of specific hydrophobic interactions that help to reorient the molecule for optimal contacts with the membrane. The interactions involved in the second step of "phospholipid bilayer interactions" primarily implicate Trp35 and the nonpolar acyl tails of the phospholipid bilayer. Our NMR data clearly show that the side chain of Trp35 is unaffected by the trisaccharide interaction and retains its unusually high solvent exposure. Therefore, it is a good candidate for this role, which is probably more important than its involvement in heparin recognition. Moreover, NMR and fluorescence quenching data demonstrated its crucial role in the interaction with micelles and liposomes,[32,48] and a depth of ∼9 Å was estimated for its partial penetration into the membrane bilayer.[48] Finally, a last step of "membrane destabilization" would take place in which these interactions would trigger series of events leading to the disruption of the cell membrane producing the lysis and cell death.[16]

The membrane destabilization and cytotoxic mechanism proposed here parallels that proposed for the bactericidal action.[49,50] Other models, based on experimental data with heparin derivatives, have been proposed for the interaction of several proteins with membranes. Similarly to ECP, in the case of the cobra cardiotoxin,[51] the interaction with a hexasaccharide induces conformational changes in the protein near its membrane binding loops that would promote hydrophobic protein−lipid interaction. In Anexin V, a protein that contains two heparin binding sites located in opposite surfaces of the protein, membrane phospholipids would displace heparin from one of the binding sites favoring membrane adherence.[52] In our model, the interaction with the phospholipids of the membrane and the heparin molecules should occur in the same face of the protein surface, and the release of heparin from the binding site is not required for interaction with the phospholipid bilayer.

Apart from the limitations of the model, given the importance of protein-GAG interactions, the information at the molecular level provided by the structure of ECP with the trisaccharide-heparin mimetic reported here is highly valuable for the drug design field with potential applications to the discovery and rational design of novel and highly specific glycotherapeutic agents that target disease-related protein-HS interactions. Still, open questions remain on how specific the recognition is in terms of the carbohydrate and the minimal oligosaccharide length necessary to trigger the cytotoxicity.

Different roles for cell surface GAGs binding have been reported in the literature: increasing the protein local concentration for modulation of receptor interaction and activation,[53,54] protein activation by inducing conformational changes,[55] and promoting protein/receptor dimerization by binding to multiple molecules.[44] According to our model, the plausible role for heparin/HS GAGs in the cytotoxicity of ECP would be to promote the sequestration of ECP molecules on the cell surface, increasing the local protein concentration and inducing its aggregation to facilitate specific interactions with the phospholipid bilayer that lead to the membrane disintegration.

METHODS

Trisaccharide Heparin Mimetic Synthesis. The trisaccharide heparin mimetic used in this study is a small and homogeneous chemically synthesized heparin fragment that includes the basic repeating disaccharide unit building block (IdoA-GlcNS) of native heparin: *O*-iPr-α-D-GlcNS6S-α(1−4)-L-IdoA2S-α(1−4)-D-GlcNS6S with α(1−4) linkages. The synthesis was performed using a stepwise synthetic approach for the chain using protected saccharides followed by deprotection and sulfation once the main chain was formed.[56,57] The nomenclature of **A** for the GlcNS6S ring at the reducing end, **B** for the IdoA2S ring in the center of the trisaccharide, and **C** for the GlcNS6S ring at the nonreducing end is used throughout the text.

Expression and Purification of Recombinant ECP. The recombinant protein was expressed in *Escherichia coli* BL21(DE3) cells (Novagen, USA) using the pET11c expression vector and a rich medium (unlabeled ECP) or a minimal medium (uniformly labeled ECP) containing either $^{15}NH_4Cl$ as the sole source for nitrogen (^{15}N-ECP) or $^{15}NH_4Cl$ and $^{13}C_6$-glucose as the sole sources for nitrogen and carbon (^{13}C,^{15}N-ECP), respectively. The protein was purified from inclusion bodies by an FPLC cation exchange chromatography using a Resource S column (Pharmacia) followed by an HPLC reverse phase chromatography using a Vydac C4 column. The enzymatic activity of recombinant ECP was tested as previously reported.[58]

NMR Spectroscopy. The samples of the ECP-trisaccharide heparin mimetic complex were prepared by mixing the protein with a slight excess of the carbohydrate to ensure that most of the protein remained complexed in 100 mM potassium phosphate buffer, pH 4.0. The final protein concentration for NMR experiments was ∼0.5 mM. To prevent complex precipitation upon addition of the carbohydrate, the salt concentration was increased in the sample solution up to ∼300 mM KCl.

The assignment of the free and bound trisaccharide (Supporting Tables S2, S3, and S4) and the resonance and NOE assignments of the ECP-carbohydrate complex were obtained by standard NOE-based assignment methodology and by comparison with the previously assigned spectra of the free protein in similar conditions[23] (see Supporting Information).

Structure Calculation. The procedure followed for the determination of the structure of the ECP-trisaccharide heparin mimetic complex is described in the Supporting Information and comprises standard automated CYANA protocols based on calibrated distance constraints from experimental NOEs, docking and molecular dynamic protocols.

Determination of Binding Affinities. The binding affinity was determined from chemical shift perturbation data. Titration curves were obtained by plotting chemical shift changes as a function of the different carbohydrate/protein ratios used (0:1, 0.5:1, 1:1, 1.5:1, 2:1). Nonlinear least-squares fits to a 1:1 binding model were performed with the dissociation binding constant (K_d) and the maximum chemical shift change as the fitted parameters. Since last points of the titration are reaching saturation, the K_d values calculated can be regarded as accurate. To map the interaction surface, average amide ^{15}N and ^{1}H chemical shift perturbations were calculated according to $\delta_{av} = ((\Delta\delta^2_{NH} + \Delta\delta^2_N/25)/2)^{0.5}$.

ASSOCIATED CONTENT

Supporting Information

Experimental procedures and comparison of the ECP-trisaccharide heparin mimetic complex with the sulfate-crystallized structure and docking predictions. This material is available free of charge *via* the Internet at http://pubs.acs.org.

Accession Codes

Chemical shifts have been deposited in the BMRB, accession number 18596, and the coordinates of the ECP complex structures in the PDB, accession number 2LVZ.

AUTHOR INFORMATION

Corresponding Author

*E-mail: mbruix@iqfr.csic.es.

Notes

The authors declare no competing financial interest.

■ ACKNOWLEDGMENTS

This work was supported by projects CTQ2008-0080, CTQ2011-22514, CTQ2009-08536, and CTQ2009-07168 from the Spanish Ministerio de Economía y Competitividad and P07-FQM-02969 from the Junta de Andalucía. J.A. acknowledges financial support from the Spanish Ramón y Cajal program. We thank D.V. Laurents for English style suggestions. We thank the Supercomputing Centre of Galicia (CESGA) for computation resources.

■ REFERENCES

(1) Ardelt, W., Ardelt, B., and Darzynkiewicz, Z. (2009) Ribonucleases as potential modalities in anticancer therapy. *Eur. J. Pharmacol. 625*, 181−189.
(2) Rosenberg, H. F. (2008) RNase A ribonucleases and host defense: an evolving story. *J. Leukocyte Biol. 83*, 1079−1087.
(3) Sorrentino, S. (2010) The eight human "canonical" ribonucleases: molecular diversity, catalytic properties, and special biological actions of the enzyme proteins. *FEBS Lett. 584*, 2194−2200.
(4) Boix, E., Salazar, V. A., Torrent, M., Pulido, D., Nogués, M. V., and Moussaoui, M. (2012) Structural determinants of the eosinophil cationic protein antimicrobial activity. *Biol. Chem. 393*, 801−815.
(5) Malik, A., and Batra, J. K. (2012) Antimicrobial activity of human eosinophil granule proteins: involvement in host defence against pathogens. *Crit. Rev. Microbiol. 38*, 168−181.
(6) Bystrom, J., Amin, K., and Bishop-Bailey, D. (2011) Analysing the eosinophil cationic protein-a clue to the function of the eosinophil granulocyte. *Respir. Res. 12*, 10.
(7) Gupta, S. K., Haigh, B. J., Griffin, F. J., and Wheeler, T. T. (2012) The mammalian secreted RNases: Mechanisms of action in host defence. *Innate Immun.*, DOI: 10.1177/1753425912446955.
(8) Hogan, S. P., Rosenberg, H. F., Moqbel, R., Phipps, S., Foster, P. S., Lacy, P., Kay, A. B., and Rothenberg, M. E. (2008) Eosinophils: Biological properties and role in health and disease. *Clin. Exp. Allergy 38*, 709−750.
(9) Navarro, S., Boix, E., Cuchillo, C. M., and Nogués, M. V. (2010) Eosinophil-induced neurotoxicity: The role of eosinophil cationic protein/RNase 3. *J. Neuroimmunol. 227*, 60−70.
(10) Domachowske, J. B., Dyer, K. D., Adams, A. G., Leto, T. L., and Rosenberg, H. F. (1998) Eosinophil cationic protein/RNase 3 is another RNase A-family ribonuclease with direct antiviral activity. *Nucleic Acid Res. 24*, 3507−3513.
(11) Rosenberg, H. F. (1995) Recombinant human eosinophil cationic protein. Ribonuclease activity is not essential for cytotoxicity. *J. Biol. Chem. 270*, 7876−7881.
(12) Motojima, S., Frigas, E., Loegering, D. A., and Gleich, G. J. (1989) Toxicity of eosinophil cationic proteins for guinea pig tracheal epithelium in vitro. *Am. Rev. Respir. Dis. 139*, 801−805.
(13) Hohlfeld, J. M., Schmiedl, A., Erpenbeck, V. J., Venge, P., and Krug, N. (2004) Eosinophil cationic protein alters pulmonary surfactant structure and function in asthma. *J. Allergy Clin. Immunol. 113*, 496−502.
(14) Maeda, T., Kitazoe, M., Tada, H., de Llorens, R., Salomom, D. S., Ueda, M., Yamada, H., and Seno, M. (2002) Growth inhibition of mammalian cells by eosinophil cationic protein. *Eur. J. Biochem. 269*, 306−316.
(15) Carreras, E., Boix, E., Navarro, S., Rosenberg, H. F., Cuchillo, C. M., and Nogués, M. V. (2005) Surface-exposed amino acids of eosinophil cationic protein play a critical role in the inhibition of mammalian cell proliferation. *Mol. Cell. Biochem. 272*, 1−7.
(16) Navarro, S., Aleu, J., Jiménez, M., Boix, E., Cuchillo, C. M., and Nogués, M. V. (2008) The cytotoxicity of eosinophil cationic protein/ribonuclease 3 on eukaryotic cell lines takes place through its aggregation on the cell membrane. *Cell. Mol. Life Sci. 65*, 324−337.
(17) Jacobsen, E. A., Helmers, R. A., Lee, J. J., and Lee, N. A. (2012) The expanding role(s) of eosinophils in health and disease. *Blood*,.
(18) Wechsler, M. E., Fulkerson, P. C., Bochner, B. S., Gauvreau, G. M., Gleich, G. J., Henkel, T., Kolbeck, R., Mathur, S. K., Ortega, H., Patel, J., Prussin, C., Renzi, P., Rothenberg, M. E., Roufosse, F., Simon, D., Simon, H. U., Wardlaw, A., Weller, P. F., and Klion, A. D. (2012) Novel targeted therapies for eosinophilic disorders. *J. Allergy Clin. Immuno. 130*, 563−571.
(19) Ahmed, T., Smith, G., Vlahov, I., and Abraham, W. M. (2012) Inhibition of allergic airway responses by heparin derived oligosaccharides: identification of a tetrasaccharide sequence. *Respir. Res. 13*, 6.
(20) Fan, T. C., Chang, H. T., Chen, I. W., Wang, H. Y., and Chang, M. D. T. (2007) A heparan sulfate-facilitated and raft-dependent macropinocytosis of eosinophil cationic protein. *Traffic 8*, 1778−1795.
(21) Fuchs, S. M., and Raines, R. T. (2006) Internalization of cationic peptides: the road less (or more?) traveled. *Cell. Mol. Life Sci. 63*, 1819−1822.
(22) Chao, T. Y., Lavis, L. D., and Raines, R. T. (2010) Cellular uptake of ribonuclease A relies on anionic glycans. *Biochemistry 49*, 10666−10673.
(23) Laurents, D. V., Bruix, M., Jiménez, M. A., Santoro, J., Boix, E., Moussaoui, M., Nogués, M. V., and Rico, M. (2009) The 1H, 13C, 15N resonance assignment, solution structure, and residue level stability of eosinophil cationic protein/RNase 3 determined by NMR spectroscopy. *Biopolymers 91*, 1018−1028.
(24) Boix, E., Leonidas, D. D., Nikolovski, Z., Nogués, M. V., and Cuchillo, C. M. (1999) Crystal structure of eosinopkil cationic protein at 2.4 Å resolution. *Biochemistry 38*, 16794−16801.
(25) Mallorquí-Fernández, G., Pous, J., Peracaula, R., Aymani, J., Maeda, T., Tada, H., Yamada, H., Seno, M., de Llorens, R., Gomis-Rüth, F. X., and Coll, M. (2000) Three-dimensional crystal structure of human eosinophil cationic protein (RNase 3) at 1.75 Å resolution. *J. Mol. Biol. 300*, 1297−1307.
(26) Boix, E., Pulido, D., Moussaoui, M., Nogués, M. V., and Russi, S. (2012) The sulfate-binding site structure of the human eosinophil cationic protein as revealed by a new crystallographic form. *J. Struct. Biol. 179*, 1−9.
(27) Mohan, C. G., Boix, E., Evans, H. R., Nikolovski, Z., Nogués, M. V., Cuchillo, C. M., and Acharya, K. R. (2002) The crystal structure of eosinophil cationic protein in complex with 2′,5′-ADP at 2.0 Å resolution reveals the details of the ribonucleolytic active site. *Biochemistry 41*, 12100−12106.
(28) Canales, A., Lozano, R., López-Méndez, B., Angulo, J., Ojeda, R., Nieto, P. M., Martín-Lomas, M., Giménez-Gallego, G., and Jiménez-Barbero, J. (2006) Solution NMR structure of a human FGF-1 monomer, activated by a hexasaccharide heparin-analogue. *FEBS J. 273*, 4716−4727.
(29) Bishop, J. R., Schuksz, M., and Esko, J. D. (2007) Heparan sulphate proteoglycans fine-tune mammalian physiology. *Nature 446*, 1030−1037.
(30) Gandhi, N. S., and Mancera, R. L. (2010) Heparin/heparan sulphate-based drugs. *Drug Discovery Today 15*, 1058−1069.
(31) Fan, T. C., Fang, S. L., Hwang, C. S., Hsu, C. Y., Lu, X. A., Hung, S. C., Lin, S. C., and Chang, M. D. T. (2008) Characterization of molecular interactions between eosinophil cationic protein and heparin. *J. Biol. Chem. 283*, 25468−25474.
(32) García-Mayoral, M. F., Moussaoui, M., de la Torre, B. G., Andreu, D., Boix, E., Nogués, M. V., Rico, M., Laurents, D. V., and Bruix, M. (2010) NMR structural determinants of eosinophil cationic protein binding to membrane and heparin mimetics. *Biophys. J. 98*, 2702−2711.
(33) Skinner, R., Abrahams, J. P., Whisstock, J. C., Lesk, A. M., Carrell, R. W., and Wardell, M. R. (1997) The 2.6 Å structure of antithrombin indicates a conformational change at the heparin binding site. *J. Mol. Biol. 266*, 601−609.
(34) Angulo, J., Nieto, P. M., and Martín-Lomas, M. (2003) A molecular dynamics description of the conformational flexibility of the L-iduronate ring in glycosaminoglycans. *Chem. Commun. 13*, 1512−1513.

(35) Mulloy, B., Forster, M. J., Jones, C., and Davies, D. B. (1993) N.m.r. and molecular-modelling studies of the solution conformation of heparin. *Biochem. J. 293*, 849−858.
(36) Mulloy, B., and Forster, M. J. (2000) Conformation and dynamics of heparin and heparan sulfate. *Glycobiology 10*, 1147−1156.
(37) Sue, S. C., Brisson, J. R., Chang, S. C., Huang, W. N., Lee, S. C., Jarrell, H. C., and Wu, W. (2001) Structures of heparin-derived disaccharide bound to cobra cardiotoxins: context-dependent conformational change of heparin upon binding to the rigid core of the three-fingered toxin. *Biochemistry 40*, 10436−10446.
(38) Faham, S., Hileman, R. E., Fromm, J. R., Linhardt, R. J., and Rees, D. C. (1996) Heparin structure and interactions with basic fibroblast growth factor. *Science 271*, 1116−1120.
(39) Tjong, S. C., Chen, T. S., Huang, W. N., and Wu, W. (2007) Structures of heparin-derived tetrasaccharide bound to cobra cardiotoxins: heparin binding at a single protein site with diverse side chain interactions. *Biochemistry 46*, 9941−9952.
(40) Torrent, M., Nogués, M. V., and Boix, E. (2011) Eosinophil cationic protein (ECP) can bind heparin and other glycosaminoglycans through its RNase active site. *J. Mol. Recognit. 24*, 90−100.
(41) Nieto, L., Canales, A., Giménez-Gallego, G., Nieto, P. M., and Jiménez-Barbero, J. (2011) Conformational selection of the AGA*IA_M heparin pentasaccharide when bound to the fibroblast growth factor receptor. *Chemistry 17*, 11204−11209.
(42) Pineda-Lucena, A., Jiménez, M. A., Nieto, J. L., Santoro, J., Rico, M., and Giménez-Gallego, G. (1994) 1H-NMR assignment and solution structure of human acidic fibroblast growth factor activated by inositol hexasulfate. *J. Mol. Biol. 242*, 81−98.
(43) Swaminathan, G. J., Myszka, D. G., Katsamba, P. S., Ohnuki, L. E., Gleich, G. J., and Acharya, K. R. (2005) Eosinophil-granule major basic protein, a C-type lectin, binds heparin. *Biochemistry 44*, 14152−14158.
(44) Xue, Y., Lee, S., and Ha, Y. (2011) Crystal structure of amyloid precursor-like protein 1 and heparin complex suggests a dual role of heparin in E2 dimerization. *Proc. Natl. Acad. Sci. U.S.A. 108*, 16229−16234.
(45) Asensio, J. L., Ardá, A., Cañada, F. J., and Jiménez-Barbero, J. (2012) Carbohydrate-aromatic interactions. *Acc. Chem. Res.*, DOI: 10.1021/ar300024d.
(46) Mikhailov, D., Linhardt, R. J., and Mayo, K. H. (1997) NMR solution conformation of heparin-derived hexasaccharide. *Biochem. J. 328*, 51−61.
(47) Carreras, E., Boix, E., Rosenberg, H. F., Cuchillo, C. M., and Nogués, M. V. (2003) Both aromatic and cationic residues contribute to the membrane-lytic and bactericidal activity of eosinophil cationic protein. *Biochemistry 42*, 6636−6644.
(48) Torrent, M., Cuyas, E., Carreras, E., Navarro, S., López, O., de la Maza, A., Nogués, M. V., Reshetnyak, Y. K., and Boix, E. (2007) Topography studies on the membrane interaction mechanism of the eosinophil cationic protein. *Biochemistry 46*, 720−733.
(49) Lehrer, R. I., Szklarek, D., Barton, A., Ganz, T., Hamann, K. J., and Gleich, G. J. (1989) Antibacterial properties of eosinophil major basic protein and eosinophil cationic protein. *J. Immunol. 142*, 4428−4434.
(50) Torrent, M., Badia, M., Moussaoui, M., Sánchez, D., and Nogués, M. V. (2010) Comparison of human RNase 3 and RNase 7 bactericidal action at the Gram-positive bacterial cell wall. *FEBS J. 277*, 1713−1725.
(51) Sue, S. C., Chien, K. Y., Huang, W. N., Abraham, J. K., Chen, K. M., and Wu, W. (2002) Heparin binding stabilizes the membrane-bound form of cobra cardiotoxin. *J. Biol. Chem. 227*, 2666−2673.
(52) Capila, I., Hernáiz, M. J., Mo, Y. D., Mealy, T. R., Campos, B., Dedman, J. R., Linhardt, R. J., and Seaton, B. A. (2001) Annexin V-heparin oligosaccharide complex suggests heparan sulfate-mediated assembly on cell surfaces. *Structure 9*, 57−64.
(53) Kuschert, G. S., Coulin, F., Power, C. A., Proudfoot, A. E., Hubbard, R. E., Hoogewerf, A. J., and Wells, T. N. (1999) Glycosaminoglycans interact selectively with chemokines and modulate receptor binding and cellular responses. *Biochemistry 37*, 11193−11201.
(54) Murphy, J. W., Cho, Y., Sachpatzidis, A., Fan, C., Hodsdon, M. E., and Lolis, E. (2007) Structural and functional basis of CXCL12 (stromal cell-derived factor-1a) binding to heparin. *J. Biol. Chem. 282*, 10018−10027.
(55) Evans, D. L., Marshall, C. J., Christey, P. B., and Carrell, R. W. (1992) Heparin binding site, conformational change, and activation of antithrombin. *Biochemistry 31*, 12629−12642.
(56) de Paz, J. L., Angulo, J., Lassaletta, J. M., Nieto, P. M., Redondo-Horcajo, M., Lozano, R. M., Giménez-Gallego, G., and Martín-Lomas, M. (2001) The activation of fibroblast growth factors by heparin: synthesis, structure, and biological activity of heparin-like oligosaccharides. *ChemBioChem 2*, 673−685.
(57) Muñoz-García, J. C., López-Prados, J., Angulo, J., Díaz-Contreras, I., Reichardt, N. C., de Paz, J. L., Martín-Lomas, M., and Nieto, P. M. (2012) Effect of the substituents of neighbour ring in the conformational equilibrium of iduronate in heparin-like trisaccharides. *Chemistry*, DOI: 10.1002/chem.201202770.
(58) Boix, E., Nikolovski, Z., Moiseyev, G. P., Rosenberg, H. F., Cuchillo, C. M., and Nogués, M. V. (1999) Kinetic and product distribution analysis of human eosinophil cationic protein indicates a subsite arrangement that favors exonuclease-type activity. *J. Biol. Chem. 274*, 15605−15614.